Comparison of X-Ray Attenuation Performance, Antimicrobial Properties, and Cytotoxicity of Silicone-Based Matrices Containing Bi_2O_3, PbO, or Bi_2O_3/PbO Nanoparticles

Baharak Divband (PhD)[1,2], Zahraa Haleem Al-qaim (PhD)[3], Falah H. Hussein (PhD)[4], Davood Khezerloo (PhD)[5,6], Nahideh Gharehaghaji (PhD)[5,6]*

[1]Dental and Periodontal Research Center, Tabriz University of Medical Sciences, Tabriz, Iran
[2]Inorganic Chemistry Department, Chemistry Faculty, University of Tabriz, Tabriz, Iran
[3]Anesthesia Techniques Department, College of Health and Medical Techniques, Al_Mustaqbal University, 51001, Babylon, Iraq
[4]College of Pharmacy, University of Babylon, Iraq
[5]Department of Radiology, Faculty of Allied Medical Sciences, Tabriz University of Medical Sciences, Tabriz, Iran
[6]Medical Radiation Sciences Research Center, Tabriz University of Medical Sciences, Tabriz, Iran

ABSTRACT

Background: Application of the nanomaterials to preparing X-ray shields and successfully treating multiresistant microorganisms has attracted great attention in modern life.

Objective: This study aimed to prepare flexible silicone-based matrices containing Bi_2O_3, PbO, or Bi_2O_3/PbO nanoparticles and select a cost-effective, cytocompatible, and antibacterial/antifungal X-ray shield in clinical radiography.

Material and Methods: In this experimental study, we prepared the nanoparticles by the modified biosynthesis method and fabricated the X-ray shields containing 20 wt% of the nanoparticles. The X-ray attenuation percentage and Half Value Layer (HVL) of the shields were investigated for the photon energies in the range of 40-100 kVp in clinical radiography. The antibacterial/antifungal activities of the shields were evaluated using a colony count method for the gram-negative (*Escherichia coli*), and gram-positive (*Enterococcus faecalis*) bacteria, and Candida albicans fungus. The shield toxicity was investigated on A549 cells.

Results: The highest X-ray attenuation percentage and the lowest HVL were obtained using the shield containing Bi_2O_3 nanoparticles. Although all shields displayed antimicrobial activity, the shield containing Bi_2O_3/PbO nanoparticles showed the most effective reduction in the colony counts. Both X-ray shields containing nano Bi_2O_3 and Bi_2O_3/PbO demonstrated high cytocompatibility on A549 cells at a concentration as high as 500 µg/ml. The shield with PbO nanoparticles was also cytocompatible at a concentration of 50 µg/ml.

Conclusion: The best X-ray attenuation performance is attributed to the silicone-based matrix with nano Bi_2O_3; however, the flexible shield with Bi_2O_3/PbO nanoparticles can be cost-effective and cytocompatible with the best antibacterial/antifungal properties.

Citation: Divband B, Haleem Al-qaim Z, Hussein FH, Khezerloo D, Gharehaghaji N. Comparison of X-Ray Attenuation Performance, Antimicrobial Properties, and Cytotoxicity of Silicone-Based Matrices Containing Bi_2O_3, PbO, or Bi_2O_3/PbO Nanoparticles. *J Biomed Phys Eng.* 2024;14(6):533-546. doi: 10.31661/jbpe.v0i0.2403-1736.

Keywords

X-Rays; Shield; Half Value Layer; Antimicrobial Activity; Bi_2O_3/PbO; Nanoparticles; Toxicity

Introduction

Ionizing radiations are widely used in a variety of biomedical fields, including medical imaging and radiotherapy [1]. However, they can cause ionizing radiation-induced cancer, especially during repeated exposures to radiation [2, 3]. Among different types of ionizing radiation, X-ray has an important role in the radiology and diagnosis

*Corresponding author:
Nahideh Gharehaghaji
Department of Radiology, Faculty of Allied Medical Sciences, Tabriz University of Medical Sciences, Tabriz, Iran
E-mail: gharehaghaji@gmail.com

Received: 11 March 2024
Accepted: 14 August 2024

of diseases [4]. Patients who undergo X-ray examinations receive both primary and scatter radiations, and medical staff are exposed to scatter radiations [5]. Therefore, the development of efficient X-ray shields to protect sensitive organs is necessary. Commercial shields constructed from lead (Pb) and bismuth (Bi) compounds in different sizes are routinely utilized in radiology centers and clinics, due to the best absorption of X-rays using materials with high atomic number and high density [6, 7].

Lead is the most common material used as a radiation shield due to its high density, easy fabrication, availability, and stability level [8]. Lead with an atomic number of 82 has a high ability to absorb X-rays. However, the heaviness of lead aprons especially in long-term use for radiation workers, its low flexibility, which causes damage to the shield structure, and its toxicity have led to attention being drawn to mixing lead with other metals or its replacement with other materials for X-ray shielding [5, 9-11]. Bismuth with an atomic number of 83 is one of these materials that is used as a commercial X-ray shield. Compared to lead, bismuth has a higher absorption cross-section and lower toxicity. In addition, the softness of bismuth makes it an X-ray shield with appropriate flexibility [12, 13]; however, bismuth has a higher raw material cost than lead [14]. Therefore, lead shields are still commonly used in radiology centers.

In recent years, nanostructures have been suggested for use in X-ray shields due to their good mechanical ability, lightweight, and durability [15, 16]. Nanosized materials show unique properties that differ from bulk materials [17]. The high surface-to-volume ratio of nanomaterials provides more interaction of radiation with matter [1]. So far, the X-ray protection ability of different shields containing nanomaterials has been investigated, which can be pointed out to bismuth oxide (Bi_2O_3) [18-23], copper oxide (CuO) [15], tungsten oxide (WO_3) [9, 18], gadolinium oxide (Gd_2O_3) [24], and lead oxide (PbO) nanoparticles [18]. Additionally, the effect of micro and nano-size particles of some materials was compared on the X-ray absorption [9, 15, 18, 23, 25].

Among different nanoparticles used in the X-ray shields, Bi_2O_3 nanoparticles have been widely investigated for X-ray shielding [18-23]. Also, comparative studies were done between the shields containing Bi_2O_3 nanoparticles and other nanomaterials. Asari Shik et al. compared the X-ray shielding ability of the Emulsion of Poly Vinyl Chloride (EPVC) composites containing Bi_2O_3, WO_3, or PbO micro or nanoparticles. The results showed that the X-ray attenuation of the composites containing nanoparticles was better than that of those with microparticles of the same materials. In addition, the composites with Bi_2O_3 or PbO nanoparticles demonstrated the highest X-ray attenuation and their performances were almost identical. However, the cytotoxicity and antimicrobial activities of the composites with Bi_2O_3 or PbO nanoparticles and the shielding ability of a shield containing a mixture of these nanoparticles were not investigated [18]. Mixing two materials with different chemical or physical characteristics can make a new composite with different properties from each one [19]. Moreover, Özdemir et al. used an Ethylene Propylene Diene Terpolymer (EPDM) elastomer matrix with surface-modified PbO nanoparticles as the functional material for gamma ray shielding. Besides, the effect of the shield containing 20% PbO+40% Bi_2O_3 was investigated on the X-ray attenuation. However, they only performed the radiography with 80 kV and 100 mAs [26].

The developed X-ray shields may have toxicity, which can affect the consumers' health. Hospital infections can affect the medical staff who are exposed to different types of bacteria and fungi. Thus, developing the non-toxic antimicrobial X-ray shields is essential [27]. Nanomaterials, such as bismuth oxide and lead oxide have antimicrobial activities, increasing their efficiency in X-ray shields. The surface

of the X-ray shields containing nanomaterials is rough, providing favorable sites for colonization of the microbes. Since X-ray protective shields are used for different patients undergoing radiographic procedures, transmission of bacterial and fungal diseases from one patient to another is possible. Shields with antibacterial/antifungal properties can prevent microbial disease transmission. Hashmi et al. investigated the toxicity of the polyaniline reinforced with hybrid graphene oxide-iron tungsten nitride flakes and their antibacterial/antifungal activities against gram-negative bacteria (*E. coli* and *Pseudomonas aeruginosa*), gram-positive bacteria (*Staphylococcus aureus* and *Enterococcus faecalis*), and yeast (*Candida*). Their results indicated the non-toxic effect and the microorganism's removing property of the shields [27]. Verma et al. showed that the nanocomposite containing polygonal-shaped Bi_2O_3 nanoparticles in carbon nanotubes has antibacterial activity in addition to its X-ray shielding effect. They studied the antibacterial activity of this dried gel-like hybrid nanocomposite against *Lactobacillus plantarum* and *Enterococcus faecalis* as gram-positive bacteria using a modified disc diffusion assay [20]. The results of Hernandez-Delgadillo et al. study showed inhibition of *Candida albicans* growth using the aqueous colloidal Bi_2O_3 nanoparticles [28]. The antibacterial effect of the Bi_2O_3, Bi_2O_3/GO and Bi_2O_3/CuO/GO nanocomposites against *Escherichia coli* and *Pseudomonas* as gram-negative and *Bacillus cereus* and *Staphylococcus aureus* as gram-positive bacteria was confirmed in Qayyum et al. study [29]. The Bi_2O_3 nano-flakes were introduced as antibacterial agent with the activity against multidrug-resistant *Escherichia coli* and Methicillin-resistant Staphylococcus aureus bacteria [14]. A gradual decrease in the growth of *Bacillus cereus* and *Pseudomonas aeruginosa* bacteria was shown by increasing the Bi_2O_3 nanoparticles concentration [30]. Firouzi Dalvand et al. compared the antimicrobial effect of the Bi_2O_3 nanoparticles on methicillin-resistant *Staphylococcus aureus* with the antibiotics, such as Ciprofloxacin. They concluded that it may be possible to reduce the antibiotics concentration and to use Bi_2O_3 nanoparticles in the infections treatment to decrease antibiotic resistance [31]. Further, the antibacterial activity of the lead oxide nanoparticles against *Escherichia coli* and *Staphylococcus aureus* was studied using the diffusion method [32]. Since the antimicrobial properties of bare nanoparticles compared to polymer-based matrices containing the nanoparticles will be different, investigation of the antimicrobial activity of the shields containing Bi_2O_3 or PbO nanoparticles or their mixture seems necessary.

Despite the development of lead-free shields due to lead toxicity, the results of one study that assessed the lead poisoning risk from lead shields for radiology workers showed no increased risk of lead poisoning in the workers' blood and hands. The researchers of the study concluded that "lead poisoning is unlikely to occur with high frequency in lead shield users" [33]. However, common low-cost lead shields are heavy and low flexible. Expensive alternatives with less toxicity based on heavy metal oxides (i.e. Bi_2O_3) are more effective. Therefore, preparing shields containing a mixture of nano PbO and Bi_2O_3 may be a promising cost-effective, lightweight, and flexible X-ray shield. Moreover, nanomaterials with a high surface-to-volume ratio in the shields instead of the bulk materials improve the interaction of X-ray with the matter.

This study aimed to compare the X-ray attenuation performance, cytotoxicity, and antimicrobial properties of the flexible silicone-based matrices containing Bi_2O_3, PbO, or Bi_2O_3/PbO nanoparticles (as lead-free, lead-based, and their mixture shields, respectively) to select a cost-effective, cytocompatible, and antibacterial/antifungal X-ray shield for application in clinical radiography.

In the current study, we prepared silicone-based shields containing Bi_2O_3, PbO, or Bi_2O_3/

PbO nanoparticles and investigated their performance as diagnostic X-ray shields for different radiographic tube voltages. We also investigated the cytotoxicity of the shields and their antimicrobial activities against multiresistant microorganisms to common antimicrobials, including *Escherichia coli* and *Enterococcus faecalis bacteria,* and *Candida albicans* fungus.

Material and Methods

This experimental study was conducted as following steps:

Nanoparticles preparation/nanocomposite shield construction

Preparation of nano Bi_2O_3

Nano Bi_2O_3 was prepared by a modified biosynthesis method [21, 34]. Typically, Bi $(NO_3)_3$•$5H_2O$ (0.1 mol) was dissolved in 200 ml citric acid (1 M) and heated up to 60 °C. As the next step, 50 ml of warm gelatin aqueous solution (as a capping agent) was added and stirred in the water bath (75 °C) for 4 h. Then, adding NH_4OH (2 M) led to adjusting the pH of the solution to 10. At last, the resulting yellow participant was separated from the solid-liquid mixture using high-speed centrifugation, washed several times, dried, and calcined at 500 °C for 4 h. Therefore, the Bi_2O_3 nanoparticles were resulted.

Preparation of nano PbO

Nano PbO was also prepared by a modified biosynthesis method [34]. Metallic lead (0.05 mol) was dissolved in 200 ml nitric acid (2 M), heated up to 60 °C for 3 h, and centrifuged to separate the unreacted metal particles. Then, 50 ml of warm gelatin aqueous solution (as a capping agent) was added to the clear solution of lead nitrate and stirred in the water bath (75 °C) for 4 h. At last, by adding the proper amounts of NH_4OH (2 M), the pH of the solution was adjusted to 10. Finally, the resulting brown participant was separated from the solid-liquid mixture using high-speed centrifugation, washed several times, dried, and calcined at 550 °C for 4 h. Hence, the PbO nanoparticles were obtained.

Preparation of the shields

For preparing the shields, 20 wt% of the nanoparticles (Bi_2O_3, PbO, or Bi_2O_3/PbO) and silicone (80 wt%) were mixed using a mechanical mixture for 30 min. Shields were made in 10×10 cm^2 with 1 mm thickness. Then, the resulting mixture was placed in a vacuum oven for 10 minutes at 25 °C to remove the air bubbles.

Characterization tests

Scanning Electron Microscopy (SEM) was carried out using a MIRA3 FEG-SEM instrument, equipped with Energy Dispersive X-ray (EDX) analysis for obtaining the elemental composition mapping of the samples. A small piece of each shield was attached to the typical SEM sample holder using carbon adhesive tape, and the holder was then mounted inside the chamber. For SEM images, the acceleration voltage was applied around 10 kV. The gold coating was used to avoid the charging effects due to the low conductivity of the shields. For EDX analysis, the high voltage of 10 kV was applied to produce the emission of X-rays from the samples.

X-ray attenuation measurement setup

A DRGEM (Gwangmyeong-si, Gyeonggi-do, Korea) diagnostic radiography unit was used as an X-ray source. The tube peak voltages from 40 to 100 kVp with an interval of 10 kVp, and a fixed tube current of 10 mAs were selected. The measurements were performed using a Piranha solid-state detector (RTI Group - Sweden). The detector was set at a distance of 100 cm from the focal spot. The radiation field was 20×20 cm^2 and the Automatic Exposure Control (AEC) was deactivated. The measurements were carried out

without and with the shields.

The X-ray attenuation percentage of the shields containing Bi_2O_3, PbO, or Bi_2O_3/PbO nanoparticles at each kVp was calculated based on the following Equation:

$$Attenuation\ \% = \frac{D0 - D}{D0} \times 100 \quad (1)$$

where D0 is the measured radiation dose without the shield and D is the measured radiation dose using the shield.

The values of linear attenuation coefficient (μ) and Half Value Layer (HVL) for each shield at the kVps were calculated using Equations 2 and 3, respectively, as follows:

$$\mu = -\frac{1}{X} \ln \frac{D}{D0} \quad (2)$$

$$HVL = \frac{0.693}{\mu} \quad (3)$$

where X is the shield thickness.

Antibacterial and antifungal activities

In this study, we used the standard strains of *Enterococcus faecalis* (ATCC 29212), *Escherichia coli* (ATCC 25922) and *Candida albicans* (ATCC 10239) to determine the antimicrobial activity of the shields by the colony count method.

The standard strain of *Enterococcus faecalis* was cultivated on Brain-Heart Infusion (BHI) agar for 24 h at 37 °C. After the incubation period, the standard 0.5 McFarland concentration of Enterococcus faecalis (1.5×10^8 colonies forming unit per milliliter (CFU/mL)) was prepared. In the sterile condition, for each of the wells containing the shields, 100 μL of the prepared concentration of bacteria was inoculated and incubated for 24 h at 37 °C. Several dilutions (10^{-1}, 10^{-2}, 10^{-3}, …) were prepared for counting the bacterial colonies number in each of the wells. As the next step, five μL of dilute microbial suspension was inoculated on the surface of the BHI agar plate, spread with a sterile bent-glass rod using the spread plate technique and incubated for 24 h at 37 °C. Then, the plate containing 30–300 cells was selected, the colonies number was counted, and reported in CFU/mL [35].

The same steps were also carried out for Escherichia coli, and Candida albicans.

Cytotoxicity assay

3-(4,5-dimethylthiazol- 2-yl)-2,5-diphenyl-tetrazolium bromide (MTT) assay method was carried out to investigate the cell toxicity of the shields containing Bi_2O_3, PbO, or Bi_2O_3/PbO nanoparticles on A549 (human alveolar adenocarcinoma) cells. Briefly, 2×10^4 cells/well were incubated in the 96-well plate with the supplemented cell culture medium (200 μL/well) for 24 h at the condition of 37 °C and 5% CO_2. Then, the treatment of the cells was done with 50, 100, and 500 μg/ml concentrations of the nanoparticles in the silicone matrix. The media were eliminated after incubation, and the wells were washed using PBS (pH=7.4). Measurement of the cellular proliferation was carried out by adding 50 μL of MTT solution (2 mg/mL) and 150 μL culture medium to each well. As the next step, 24 h incubation of the A549 cells was performed at 37 °C and 5% CO_2. Then, the media was removed from the wells, and 200 μL of dimethyl sulfoxide and 25 μL Sorenson solubilizer buffer were added to each well. Finally, the samples' optical absorbance was read at 570 nm wavelength by the usage of a BioTek, Bad Friedrichshall ELISA plate reader (Germany) [36].

Statistics

To ensure the reliability of the results, the X-ray attenuation measurements and the antimicrobial experiments were repeated three and six times, respectively. The statistical significance was considered using Student's t-test. A P-value<0.05 was assessed as significant.

Results

Characterization tests

The silicone-based flexible X-ray shields

containing Bi_2O_3, PbO, or Bi_2O_3/PbO nanoparticles are seen in Figure 1.

Figure 2 demonstrates the SEM images of the shields. Based on Figure 2, the shield containing Bi_2O_3 nanoparticles showed almost homogeneous structures with irregular shapes on the surface, while the matrix containing PbO nanoparticles had homogeneous structures with regular shapes on its surface. The SEM image of the shield containing Bi_2O_3/PbO nanoparticles indicated that the deposits possess agglomerated structures with irregular shapes on the surface, showing a combination of both smooth areas (silicone) and rough areas (nanoparticles).

The EDX elemental analysis results are illustrated in Figure 3, showing Si, Bi (Pb or Bi/Pb) in the structure of the shields, with an average of 54 wt% for Si, 19 wt% for O, 16 wt% for Bi (Pb or Bi/Pb) and the rest is impurity of C.

According to MAP analyses of all prepared shields, it is seen that the nanoparticles were distributed homogeneously in the silicone matrix (Figure 4).

X-ray attenuation and HVL

Figure 5 demonstrates the X-ray attenuation percentages of the shields for the tube voltages ranging from 40-100 kVp. Decreasing in the X-ray attenuation percentage with an increase in the tube voltages was seen in all shields.

As seen in Figure 5, the shield containing Bi_2O_3 nanoparticles showed the highest amounts of the X-ray attenuation percentage at all tube voltages, while the shield with PbO nanoparticles had the lowest values. There was a significant difference in the mean X-ray attenuation percentages of the shields at all tube voltages. The most significant difference was seen between the Bi_2O_3 and PbO nanoparticles containing shields (*P*-value=0.0004), while

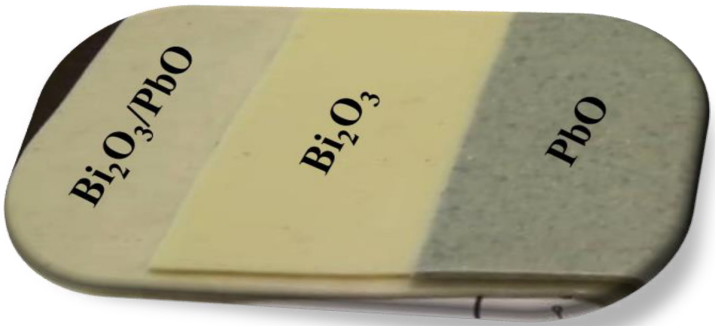

Figure 1: Digital photo of the flexible X-ray shields containing Bi_2O_3, PbO, or Bi_2O_3/PbO nanoparticles.

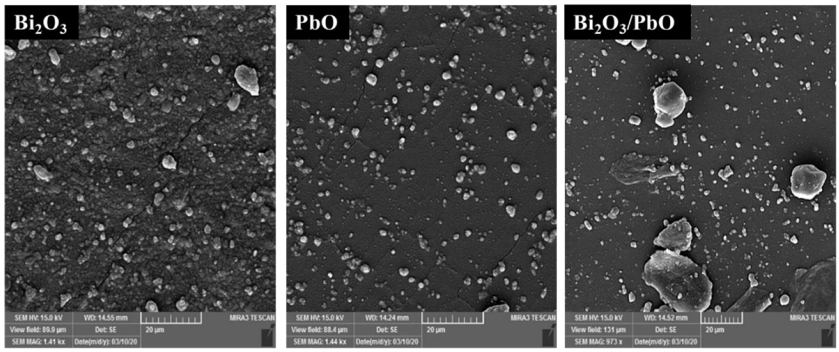

Figure 2: Scanning electron microscopy (SEM) images of the flexible X-ray shields containing Bi_2O_3, PbO, or Bi_2O_3/PbO nanoparticles.

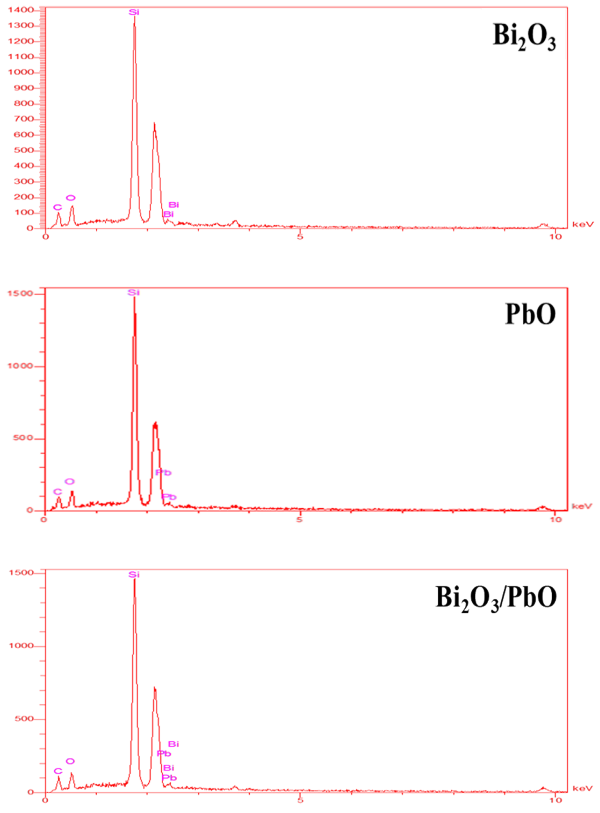

Figure 3: Energy dispersive X-ray (EDX) elemental analyses of the flexible X-ray shields containing Bi_2O_3, PbO, or Bi_2O_3/PbO nanoparticles.

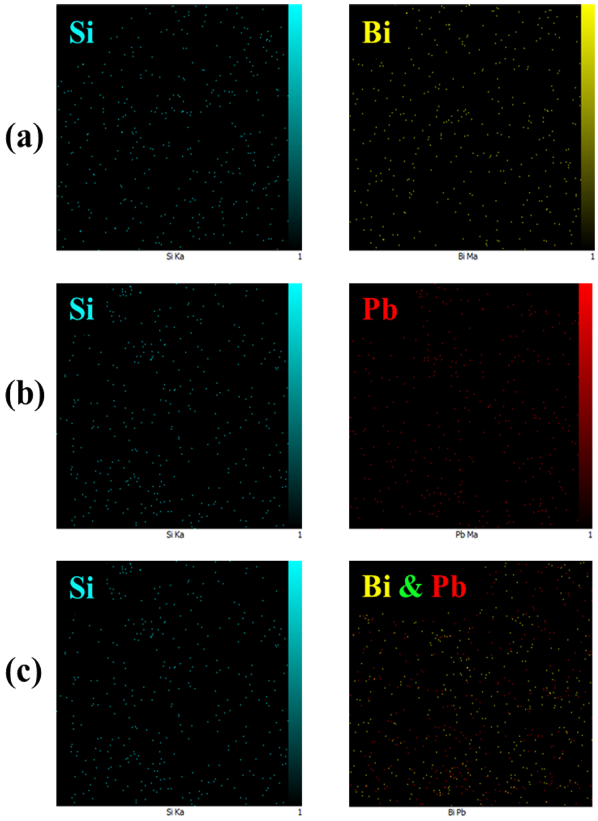

Figure 4: MAP analyses of the flexible X-ray shields containing (**a**) Bi_2O_3, (**b**) PbO, or (**c**) Bi_2O_3/PbO nanoparticles.

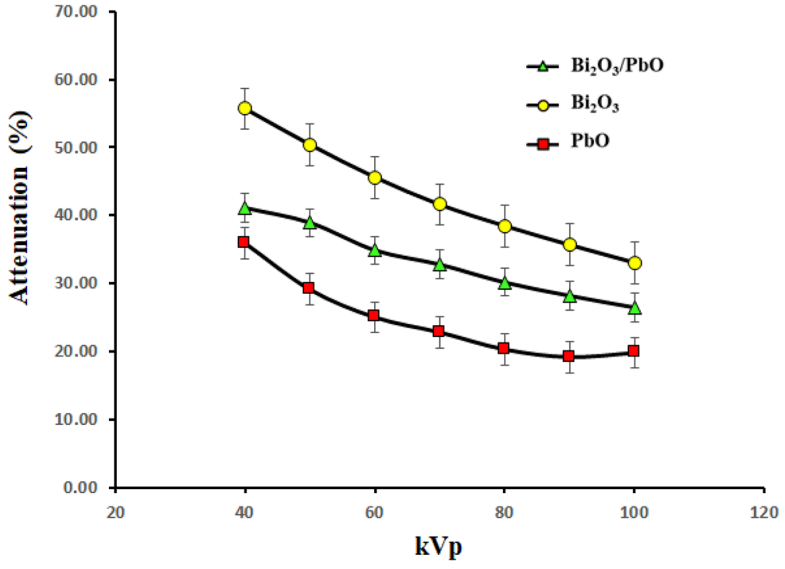

Figure 5: X-ray attenuation percentages of the flexible shields containing Bi_2O_3, PbO, or Bi_2O_3/PbO nanoparticles for tube voltages ranging from 40-100 kVp.

the difference was lower between the shields containing Bi_2O_3/PbO nanoparticles and nano PbO (*P*-value=0.016), and between nano Bi_2O_3/PbO and Bi_2O_3 nanoparticles containing shields (*P*-value=0.022).

The HVL curves of the shields containing the nanoparticles for the tube voltages ranging from 40-100 kVp are illustrated in Figure 6. The HVL values were increased as a function of the tube voltages for all shields.

Antibacterial and antifungal activities

The antimicrobial activities of the shields were investigated against gram-negative (*Escherichia coli*), and gram-positive (*Enterococcus faecalis*) bacteria and *Candida albicans* fungus. The findings confirmed the antibacterial/antifungal activities of all shields against bacteria and fungus growth (Figure 7). The silicon matrix containing Bi_2O_3/PbO nanoparticles provided the most effective reduction in the colony counts. Figure 7 also shows a greater growth inhibition effect of all shields on *Escherichia coli* than *Enterococcus faecalis*.

MTT results

Figure 8 shows the A549 cells' viability after treatment with different concentrations (50, 100, and 500 µg/ml) of the nanoparticles in the silicone matrices. A concentration-

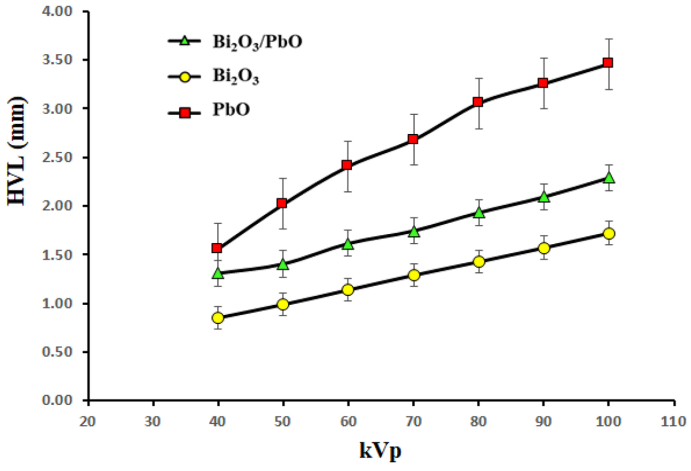

Figure 6: Half value layer (HVL) curves of the flexible X-ray shields containing Bi_2O_3, PbO, or Bi_2O_3/PbO nanoparticles for tube voltages ranging from 40-100 kVp.

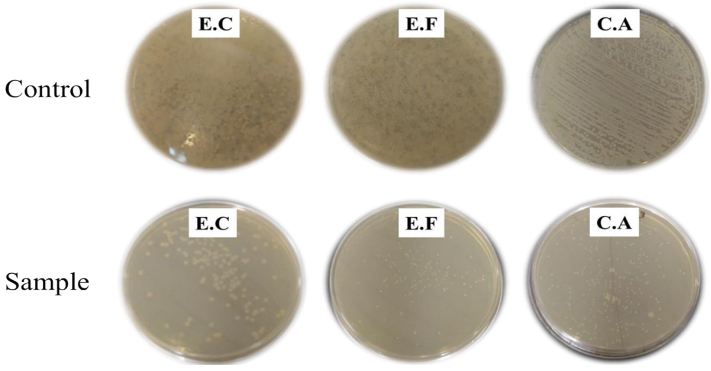

Figure 7: Antibacterial/antifungal activities of the flexible X-ray shields containing Bi_2O_3, PbO, or Bi_2O_3/PbO nanoparticles against *Escherichia coli* (*E.C*) and *Enterococcus faecalis* (*E.F*) bacteria, and *Candida albicans* (*C.A*) fungus.

dependent decrease in cell viability was seen for all shields. The cell viabilities of the shields containing Bi_2O_3 and Bi_2O_3/PbO nanoparticles were more than 80% at all concentrations. The nano Bi_2O_3 containing shield showed slightly higher cytocompatibility than the nano Bi_2O_3/PbO containing shield. Therefore, the mean cell viability difference for all concentrations was not significant between the two shields (*P*-value=0.23). The shield containing PbO nanoparticles showed more than 80% cell viability at a concentration of 50 µg/ml and about 78% and 70% at concentrations of 100 and 500 µg/ml, respectively.

Discussion

Characterization

In this work, the raw materials of the shield samples were silicone, Bi_2O_3, and PbO. Each material was weighed using a sensitive balance. The matrix was silicone as a major component in the manufacture of the shield.

SEM results showed no texture difference among different parts of each shield, confirming the uniform distribution of the nanoparticles in different parts of the matrices (as confirmed by MAP results). This is an important criterion to make sufficient radiation protection by the shields. However, according to the MAP results (Figure 4), the balk particles are related to the silicone containing the nanoparticles. It should be noted that the nanoparticles were homogenously dispersed in the balk particles.

X-ray attenuation performance and HVL

As seen in Figure 5, the X-ray attenuation percentage was decreased with increasing tube voltages for all shields, due to the photoelectric effect, which is dominant in the lower tube voltages. The photoelectric effect causes complete absorption of X-ray photons, which have energy slightly higher than the binding energy of electrons in the particular electron layers. The probability of the photoelectric effect is approximately proportional to Z^3/E^3, where Z is the atomic number of the material, absorbing the X-ray photon, and E is the energy of the X-ray photon. Since the photoelectric effect depends on the inverse of the third power of the photon energy, the X-ray attenuation percentage is higher in the lower tube voltages. Therefore, in the range of the tube voltages studied in this study (40-100 kVp), the maximum attenuation of the X-ray photons was seen at 40 kVp for all matrices containing the nanoparticles. The finding is in agreement with the results of the study related to the nano-sized bismuth oxide/epoxy-polyvinyl alcohol matrix composites investigated for general radiography [19].

The highest amount of the X-ray attenuation

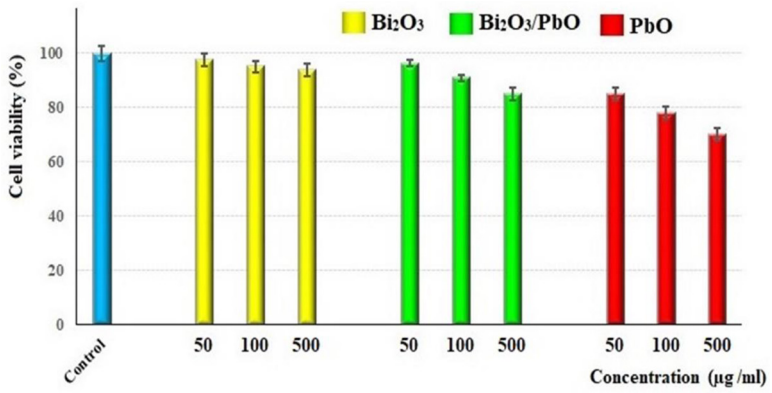

Figure 8: Cell viability of the flexible X-ray shields containing Bi_2O_3, PbO, or Bi_2O_3/PbO nanoparticles against A549 cells.

percentage at all tube voltages was obtained using the shield with Bi_2O_3 nanoparticles while the lowest values were related to the shield containing PbO nanoparticles (Figure 5). The atomic number of Pb is 82 and Bi has a Z=83. In addition, they also do not have many different binding energies at the K, L, and M electronic layers. Therefore, these findings are mainly due to the presence of two Bi atoms in the structure of the Bi_2O_3 nanoparticles, while there is only one Pb atom in the PbO nanoparticles.

It should be noted that the different crystal structure of the nano Bi_2O_3 (monoclinic) and PbO (tetragonal) and their atomic arrangement can also affect the higher X-ray attenuation percentage of the shield containing Bi_2O_3 nanoparticles. The tetragonal system has two crystallographic axes, which are equal in length (a, and b) and one (c) is different in length (shorter or longer). The axes intersect at right angles (90 degrees) to each other and form a rectangular prism. Whereas, the monoclinic system has three unequal axes, two of these crystallographic axes (a, and c) are inclined toward each other, and the other (b) is perpendicular to a, and c ($\alpha = \gamma = 90° \neq \beta$). A tetragonal crystal is uniaxial, which means when the light passes through the crystal, it appears dark in one orientation. In this regard, the monoclinic is considered a biaxial crystal. Minerals of the tetragonal system all possess a single 4-fold symmetry axis while the monoclinic crystals demonstrate a single 2-fold rotation axis and/or a single mirror plane [37]. As determined by XRD [34], the PbO has a tetragonal lattice structure featuring a pyramidal four-coordinate lead center, and the four lead–oxygen bonds have the same length [37]. Two atoms of Pb are parallel together and cover each other in the unit cell, and there are some free spaces in the unit cell; as a result, in contact with the X-ray, the X-ray can pass the lattice. In the as-prepared room temperature phase [21], α-Bi_2O_3 has a monoclinic crystal structure with a complex structure with layers of oxygen atoms and layers of bismuth atoms between them. The bismuth atoms are in two different environments, which can be described as distorted 6 and 5 coordinates, respectively [38]. In the unit cell, eight Bi atoms are distributed in the whole unit cell, which can more attenuate X-ray than PbO. Since the shield with the Bi_2O_3/PbO nanoparticles contains similar percentages (50%) of the Bi_2O_3 and PbO nanoparticles, it showed an intermediate X-ray attenuation percentage.

Figure 6 shows increasing of the HVL values as a function of the tube voltages for all shields containing the nanoparticles, due to the dominance of the photoelectric effect at lower kVps. Among the studied shields, the shield containing Bi_2O_3 nanoparticles had the lowest HVL at similar kVps. As explained earlier, this finding can be related to the presence of two Bi atoms in Bi_2O_3 and its monoclinic crystal structure. On the other hand, the highest HVL values were obtained for the shield containing PbO nanoparticles. It means that in similar tube voltages, the nano PbO shield should have the highest thickness among the shields to attenuate the X-ray photon intensity to 50% of the original values.

Comparing the results of the current study with those of Asari et al. study [18] showed some differences in the findings. They reported approximately similar X-ray attenuation performance for the EPVC composites containing Bi_2O_3 or PbO nanoparticles, while in the present study, the silicone matrix containing Bi_2O_3 nanoparticles showed a better performance compared to the matrix containing PbO nanoparticles at the same tube voltages. Their results also indicated the lowest HVL for the composite containing PbO nanoparticles, while in our study, it was related to the silicone matrix containing Bi_2O_3 nanoparticles with the highest X-ray attenuation percentage [18]. All of the silicone-based shields containing the nanoparticles in the current study showed lower HVL values than the bismuth oxide/polyester composites with different

Bi_2O_3 concentrations (0 – 6%) at 40, 50, and 60 kV. This difference is related to higher content of the particles in our shield and the nano size of the particles [39]. Also, according to the linear attenuation coefficients of the single-layered Bi_2O_3/natural rubber (NR) shields with different Bi_2O_3 contents (0 - 30 wt%), all of our shields with 20 wt% of the nanoparticles showed lower HVLs than the Bi_2O_3/NR shields at 50 and 100 keV. Only the nano PbO shield showed slightly higher HVL than the Bi_2O_3/NR shield with 30 wt% at 100 keV [40]. This is due to the nano size of the particles in our shields and their high surface-to-volume ratio, which provides more interaction of the radiation with the matter [1]. On the other hand, our shields have higher HVL than the shield containing nano tungsten trioxide (15%) and nano tin dioxide (85%) in an epoxy paint matrix at 100 kVp. However, the X-ray attenuated nanomaterials in that shield are higher than our shields [8]. The HVL of commercial bulk lead at 100 kVp (median of radiology energies range) is 0.27 mm [41]. A shield combined of tungsten (45%) and tin (55%) in a grease matrix provided HVL of 0.26 and 0.24 mm at 100 kVp for simulation and experimental studies, respectively [42]. The HVL of our nano-based lightweight and flexible shields for this energy is higher than these bulk materials. This is due to our X-ray shields containing only 20 wt% of the nanoparticles, which is much less than the X-ray attenuated materials in the shields containing the bulk materials. Besides, according to the high cytocompatibility of our nano Bi_2O_3 and Bi_2O_3/PbO shields even at high concentrations, it is possible to increase wt% of these nanomaterials in the shields to strengthen the X-ray attenuation and, consequently, to achieve lower HVLs.

Antimicrobial activities

Inhibiting the growth of multiresistant microbes has become one of the most notable concerns in modern medicine. Recently, the usage of nanomaterials as one of the novel alternatives to successfully treat multiresistant microbes has attracted great attention. In this study, Bi_2O_3, PbO, or Bi_2O_3/PbO nanoparticles were embedded in the flexible silicone matrices, and the antimicrobial activity of the prepared shields was investigated. Since the nanoparticles are exposed at the surfaces of the prepared shields, the ions on the surface can contribute to the antimicrobial properties. The high surface area of the nanoparticles and their nanoscale size provide more available sites for interaction with the microbes, enhancing their antimicrobial effect.

The results presented in Figure 7 highlight the different responses between the microbes and the prepared shields. The most effective reduction in the colony counts was provided using silicon matrix containing Bi_2O_3/PbO nanoparticles. This is due to that the nanoparticles with irregular shapes on the surface of the matrix can cause better antibacterial and antifungal performance (Figure 2). Besides, the antimicrobial synergistic effect of PbO and Bi_2O_3 nanoparticles can provide a more effective antimicrobial shield. The experimental results are in agreement with those of other studies that reported PbO [32] and Bi_2O_3 [14] nanoparticles can inhabitation of the growth of drug-resistant pathogens.

Comparing the antibacterial activities of the shields demonstrated a greater growth inhibition effect of all shields on *Escherichia coli* than *Enterococcus faecalis* (Figure 7). This finding can be due to differences in the cell wall structure between the gram-negative and gram-positive bacteria.

Cell toxicity

According to Figure 8, both X-ray shields containing Bi_2O_3 and Bi_2O_3/PbO nanoparticles showed high cytocompatibility on A549 cells. The shield containing PbO nanoparticles was also cytocompatible at a concentration of 50 µg/ml. Even at concentrations of 100 and 500 µg/ml of the PbO nanoparticles in the shield, the cell viability dropped to 78% and 70%,

showing the low toxicity of this shield in higher concentrations. Since the shields contain only 20 wt% of the nanoparticles, their distribution in the silicone matrix causes direct contact of the A549 cells with the nanoparticles in the surface of the shields, leading to inhibit of the toxic effect of the shield containing Bi_2O_3/PbO nanoparticles even at a concentration as high as 500 µg/ml and reduction the cytotoxicity of the nano PbO shield at high concentrations.

Conclusion

In this study, we prepared the silicone-based X-ray shields containing Bi_2O_3, PbO, or Bi_2O_3/PbO nanoparticles for use in clinical radiography, and investigated their physicochemical properties, X-ray attenuation performances, antibacterial/antifungal activities, and cytotoxicity. For the photon energies in the range of 40-100 kVp, the silicone-based matrix containing Bi_2O_3 nanoparticles showed the best X-ray attenuation performance with the highest X-ray attenuation percentage and the lowest HVL. However, the high price of bismuth can limit the common use of bismuth-based shields and their clinical applications. Hence, a mixture of bismuth and lead as a common cost-effective high atomic number metal ions can be favorable. The shield with Bi_2O_3/PbO nanoparticles can benefit from the advantages of both Bi_2O_3 and PbO nanoparticles. Besides, this shield demonstrated the best antibacterial/antifungal activities and high cytocompatibility. Therefore, the flexible shield containing Bi_2O_3/PbO nanoparticles with effective X-ray attenuation performance, the best antimicrobial activity, high cytocompatibility, and lower cost than the nano Bi_2O_3 shield can be considered an appropriate shield for use in clinical radiography.

Authors' Contribution

B. Divband: Methodology, Investigation, Formal analysis. D. Khezerloo, Z. Haleem Al-qaim, and FH. Hussein: Investigation, Formal analysis. N. Gharehaghaji: Funding acquisition, Project administration, Methodology, Validation, Resources. B. Divband and Z. Haleem Al-qaim have contributed to this manuscript equally. All authors contributed to the design of the study, and they wrote and reviewed the manuscript.

Ethical Approval

This study was approved by the Research Ethics Committees of Vice Chancellor in Research Affairs - Tabriz University of Medical Sciences (Ethical code: IR.TBZMED.VCR.REC.1400.489).

Funding

The Vice Chancellor for Research of Tabriz University of Medical Sciences financially supported the study (Grant No: 69159).

Conflict of Interest

None

References

1. Chandrika BM, Manjunatha HC, Sridhar KN, Ambika MR, Seenappa L, Manjunatha S, et al. Synthesis, physical, optical and radiation shielding properties of Barium-Bismuth Oxide Borate-A novel nanomaterial. *Nucl Eng Technol*. 2023;**55**:1783-90. doi: 10.1016/j.net.2023.01.
2. Moonkum N, Pilapong C, Daowtak K, Tochaikul G. Radiation Protection Device Composite of Epoxy Resin and Iodine Contrast Media for Low-Dose Radiation Protection in Diagnostic Radiology. *Polymers (Basel)*. 2023;**15**(2):430. doi: 10.3390/polym15020430. PubMed PMID: 36679309. PubMed PMCID: PMC9865924.
3. Türkaslan SS, Ugur ŞS, Türkaslan BE, Fantuzzi N. Evaluating the X-ray-Shielding Performance of Graphene-Oxide-Coated Nanocomposite Fabric. *Materials (Basel)*. 2022;**15**(4):1441. doi: 10.3390/ma15041441. PubMed PMID: 35207983. PubMed PMCID: PMC8875570.
4. Prabhu S, Bubbly SG, Gudennavar SB. X-ray and γ-ray shielding efficiency of polymer composites: choice of fillers, effect of loading and filler size, photon energy and multifunctionality. *Polym Rev*. 2023;**63**:246-88. doi: 10.1080/15583724.2022.2067867.

5. Shirkhanloo H, Safari M, Amini SM, Rashidi M. Novel semisolid design based on bismuth oxide (Bi2O3) nanoparticles for radiation protection. *Nanomed Res J.* 2017;**2**:230-8. doi: 10.22034/nmrj.2017.04.004.
6. Verma S, Sarma B, Chaturvedi K, Malvi D, Srivastava AK. Emerging graphene and carbon nanotube-based carbon composites as radiations shielding materials for X-rays and gamma rays: a review. *Compos Interfaces.* 2023;**30**:223-51. doi: 10.1080/09276440.2022.2094571.
7. Azman MN, Abualroos NJ, Yaacob KA, Zainon R. Feasibility of nanomaterial tungsten carbide as lead-free nanomaterial-based radiation shielding. *Radiat Phys Chem.* 2022;**202**:110492. doi: 10.1016/j.radphyschem.2022.110492.
8. Movahedi MM, Abdi A, Mehdizadeh AR, Dehghan N, Heidari E, Masumi Y, Abbaszadeh M. Novel paint design based on nanopowder to protection against X and gamma rays. *Indian J Nucl Med.* 2014;**29**:18-21. doi: 10.4103/0972-3919.125763. PubMed PMID: 24591777. PubMed PMCID: PMC3928744.
9. Aghaz A, Faghihi R, Mortazavi SMJ, Haghparast A, Mehdizadeh S, Sina S. Radiation attenuation properties of shields containing micro and nano WO3 in diagnostic X-ray energy range. *Int J Radiat Res.* 2016;**14**:127-31. doi: 10.18869/acadpub.ijrr.14.2.127.
10. Rahmat R, Halima N, Heryanto H, Sesa E, Tahir D. Improvement X-ray radiation shield characteristics of composite cement/Titanium dioxide (TiO2)/Barium carbonate (BaCO3): Stability crystal structure and chemical bonding. *Radiat Phys Chem.* 2023;**204**:110634. doi: 10.1016/j.radphyschem.2022.110634.
11. Safari A, Rafie P, Taeb S, Najafi M, Mortazavi SMJ. Development of Lead-Free Materials for Radiation Shielding in Medical Settings: A Review. *J Biomed Phys Eng.* 2024;**14**(3):229-44. doi: 10.31661/jbpe.v0i0.2404-1742. PubMed PMID: 39027711. PubMed PMCID: PMC11252547.
12. Aral N, Banu Nergis F, Candan C. An alternative X-ray shielding material based on coated textiles. *Text Res J.* 2016;**86**:803-11. doi: 10.1177/0040517515590409.
13. Winter H, Brown AL, Goforth AM. Bismuth-based nano-and microparticles in X-ray contrast, radiation therapy, and radiation shielding applications. *Bismuth Adv Appl Defects Charact.* 2018;**71**:1121-41. doi: 10.5772/intechopen.76413.
14. Geoffrion LD, Medina-Cruz D, Kusper M, Elsaidi S, Watanabe F, Parajuli P, et al. Bi2O3 nano-flakes as a cost-effective antibacterial agent. *Nanoscale Adv.* 2021;**3**(14):4106-18. doi: 10.1039/d0na00910e. PubMed PMID: 36132830. PubMed PMCID: PMC9417114.
15. Botelho MZ, Künzel R, Okuno E, Levenhagen RS, Basegio T, Bergmann CP. X-ray transmission through nanostructured and microstructured CuO materials. *Appl Radiat Isot.* 2011;**69**(2):527-30. doi: 10.1016/j.apradiso.2010.11.002. PubMed PMID: 21112215.
16. Shahzad K, Kausar A, Manzoor S, Rakha SA, Uzair A, Sajid M, et al. Views on radiation shielding efficiency of polymeric composites/nanocomposites and multi-layered materials: current state and advancements. *Radiation.* 2022;**3**:1-20. doi: 10.3390/radiation3010001.
17. Samadian H, Mobasheri H, Hasanpour S, Faridi-Majid R. Needleless electrospinning system, an efficient platform to fabricate carbon nanofibers. *J Nano Res.* 2017;**50**:78-89. doi: 10.4028/www.scientific.net/JNanoR.50.78.
18. Asari Shik N, Gholamzadeh L. X-ray shielding performance of the EPVC composites with micro- or nanoparticles of WO3, PbO or Bi2O3. *Appl Radiat Isot.* 2018;**139**:61-5. doi: 10.1016/j.apradiso.2018.03.025. PubMed PMID: 29723694.
19. Abunahel BM, Mustafa IS, Azman NZ. Characteristics of X-ray attenuation in nano-sized bismuth oxide/epoxy-polyvinyl alcohol (PVA) matrix composites. *Appl Phys A.* 2018;**124**:1-7. doi: 10.1007/s00339-018-2254-5.
20. Verma S, Mili M, Sharma C, Bajpai H, Pal K, Qureshi D, et al. Advanced X-ray shielding and antibacterial smart multipurpose fabric impregnated with polygonal shaped bismuth oxide nanoparticles in carbon nanotubes via green synthesis. *Green Chem Lett Rev.* 2021;**14**:272-85. doi: 10.1080/17518253.2021.1912192.
21. Mehnati P, Yousefi Sooteh M, Malekzadeh R, Divband B. Synthesis and characterization of nano Bi2O3 for radiology shield. *Nanomed J.* 2018;**5**:222-6. doi: 10.22038/NMJ.2018.05.00006.
22. Cho JH, Kim MS, Rhim JD. Comparison of radiation shielding ratios of nano-sized bismuth trioxide and molybdenum. *Radiat Eff Defects Solids.* 2015;**170**:651-8. doi: 10.1080/10420150.2015.1080703.
23. Noor Azman NZ, Musa NF, Ab Razak NN, Ramli RM, Mustafa IS, Rahman AA, Yahaya NZ. Effect of Bi2O3 particle sizes and addition of starch into Bi2O3–PVA composites for X-ray shielding. *Appl Phys A.* 2016;**122**:818. doi: 10.1007/s00339-016-0329-8.
24. Jayakumar S, Saravanan T, Philip J. Preparation,

characterization and X-ray attenuation property of Gd2O3-based nanocomposites. *Appl Nanosci.* 2017;**7**:919-31. doi: 10.1007/s13204-017-0631-6.

25. Ghasemi-Nejad M, Gholamzadeh L, Adeli R, Shirmardi SP. A comprehensive study of the antibacterial and shielding properties of micro and nano-EPVC lead-free shields. *Phys Scr*. 2022;**97**:055303. doi: 10.1088/1402-4896/ac6077.
26. Özdemir T, Güngör A, Akbay IK, Uzun H, Babucçuoglu Y. Nano lead oxide and epdm composite for development of polymer based radiation shielding material: Gamma irradiation and attenuation tests. *Radiat Phys Chem.* 2018;**144**:248-55. doi: 10.1016/j.radphyschem.2017.08.021.
27. Hashemi SA, Mousavi SM, Faghihi R, Arjmand M, Rahsepar M, Bahrani S, et al. Superior X-ray Radiation Shielding Effectiveness of Biocompatible Polyaniline Reinforced with Hybrid Graphene Oxide-Iron Tungsten Nitride Flakes. *Polymers (Basel).* 2020;**12**(6):1407. doi: 10.3390/polym12061407. PubMed PMID: 32585991. PMCID: PubMed PMC7361692.
28. Hernandez-Delgadillo R, Velasco-Arias D, Martinez-Sanmiguel JJ, Diaz D, Zumeta-Dube I, Arevalo-Niño K, Cabral-Romero C. Bismuth oxide aqueous colloidal nanoparticles inhibit Candida albicans growth and biofilm formation. *Int J Nanomedicine.* 2013;**8**:1645-52. doi: 10.2147/IJN.S38708. PubMed PMID: 23637533. PubMed PMCID: PMC3639116.
29. Qayyum A, Batool Z, Fatima M, Buzdar SA, Ullah H, Nazir A, et al. Antibacterial and in vivo toxicological studies of Bi2O3/CuO/GO nanocomposite synthesized via cost effective methods. *Sci Rep.* 2022;**12**(1):14287. doi: 10.1038/s41598-022-17332-7. PubMed PMID: 35995797. PubMed PMCID: PMC9395419.
30. Reddy BC, Seenappa L, Manjunatha HC, Vidya YS, Sridhar KN, Kumar CM, Pasha UM. Study of antimicrobial applications of Bismuth Oxide. *Mater Today Proc.* 2022;57:112-5. doi: 10.1016/j.matpr.2022.01.441.
31. Dalvand LF, Hosseini F, Dehaghi SM, Torbati ES. Inhibitory Effect of Bismuth Oxide Nanoparticles Produced by Bacillus licheniformis on Methicillin-Resistant Staphylococcus aureus Strains (MRSA). *Iran J Biotechnol.* 2018;**16**(4):e2102. doi: 10.21859/ijb.2102. PubMed PMID: 31457035. PubMed PMCID: PMC6697830.
32. Rashed HH, Fadhil FA, Hadi IH. Preparation and characterization of lead oxide nanoparticles by laser ablation as antibacterial agent. *Baghdad Sci J.* 2017;**14**(4):0801. doi: 10.21123/bsj.2017.14.4.0801.
33. Shoag JM, Michael Burns K, Kahlon SS, Parsons PJ, Bijur PE, Taragin BH, Markowitz M. Lead poisoning risk assessment of radiology workers using lead shields. *Arch Environ Occup Health.* 2020;**75**(1):60-4. doi: 10.1080/19338244.2018.1553843. PubMed PMID: 30676933.
34. Miri A, Sarani M, Hashemzadeh A, Mardani Z, Darroudi M. Biosynthesis and cytotoxic activity of lead oxide nanoparticles. *Green Chem Lett Rev.* 2018;**11**:567-72. doi: 10.1080/17518253.2018.1547926.
35. Mokhtari H, Eskandarinezhad M, Barhaghi MS, Asnaashari S, Sefidan FY, Abedi A, Alizadeh S. Comparative antibacterial effects of ginger and marjoram extract versus conventional irrigants on mature Enterococcus faecalis biofilms: An in vitro study. *J Clin Exp Dent.* 2023;**15**(4):e304-10. doi: 10.4317/jced.60081. PubMed PMID: 37152491. PubMed PMCID: PMC10155938.
36. Gharehaghaji N, Divband B. PEGylated Magnetite/Hydroxyapatite: A Green Nanocomposite for T2-Weighted MRI and Curcumin Carrying. *Evid Based Complement Alternat Med.* 2022;**2022**:1337588. doi: 10.1155/2022/1337588. PubMed PMID: 35722138. PubMed PMCID: PMC9201731.
37. Wells AF. Structural Inorganic Chemistry. 4th ed. Oxford: Clarendon Press; 1975.
38. Malmros G. The Crystal Structure of alpha-Bi2O2. *Acta Chem Scand.* 1970;**24**:384-96. doi: 10.3891/acta.chem.scand.24-0384.
39. Wahyuni F, Sakti SP, Santjojo DJ, Juswono UP. Bismuth oxide filled polyester composites for X-ray radiation shielding applications. *Polish J Environ Stud*. 2022;**3**:3985-90. doi: 10.15244/pjoes/146935.
40. Thumwong A, Darachai J, Saenboonruang K. Comparative X-ray Shielding Properties of Single-Layered and Multi-Layered Bi2O3/NR Composites: Simulation and Numerical Studies. *Polymers (Basel)*. 2022;**14**(9):1788. doi: 10.3390/polym14091788. PubMed PMID: 35566961. PubMed PMCID: PMC9099843.
41. National Council on Radiation Protection and Measurements.Structural shielding design for medical x-ray imaging facilities. Report No. 147; NCRP; 2004.
42. Aghamiri MR, Mortazavi SMJ, Tayebi M, Mosleh-Shirazi MA, Baharvand H, Tavakkoli-Golpayegani A, Zeinali-Rafsanjani B. A novel design for production of efficient flexible lead-free shields against X-ray photons in diagnostic energy range. *J Biomed Phys Eng.* 2011;**1**:17.